Sparse Deconvolution of Pulsatile Growth Hormone Secretion in Adolescents

Jon X. Genty, Md. Rafiul Amin, Natalie D. Shaw, Elizabeth B. Klerman and Rose T. Faghih

Abstract— Growth hormone (GH) is secreted by cells in the anterior pituitary on two time scales: discrete pulses over minutes that occur within a 24-hr pattern. Secretion reflects the balance of stimulatory and inhibitory inputs from the hypothalamus and is influenced by gonadal steroids, stress, nutrition, and sleep/wake states. We propose a novel approach for the analysis of GH data and use this approach to quantify (i) the timing, amplitude and the number of GH pulses and (ii) GH infusion, clearance and basal secretion (i.e., time invariant) rates, using serum GH sampled every 10 minutes during an 8-hour sleep study in 18 adolescents. In our method, we approximate hormonal secretory events by deconvolving GH data via a two-step coordinate descent approach. The first step utilizes a sparse-recovery approach to estimate the timing and amplitude of GH secretory events. The second step estimates physiological parameters. Our method identifies the timing and amplitude of GH pulses and system parameters from experimental and simulated data, with a median R^2 of 0.93, among experimental data. Recovering GH pulses and model parameters using this approach may improve the quantification of GH parameters under different physiological and pathological conditions and the design and monitoring of interventions.

Index Terms— Biomedical signal processing, deconvolution, constrained optimization, state-space methods, growth hormone, pulsatile hormones

1 Introduction

Growth hormone (GH) plays a vital role in mammalian growth and metabolism across the lifespan. GH induces linear growth in children primarily by stimulating the hepatic secretion of insulin-like growth factor 1 (IGF1), which then acts at the growth plate [1, 2]. GH also promotes protein synthesis, lipolysis and maintains glucose homeostasis [3] by acting on the liver, adipose tissue, muscles and kidney [4]. Circulating GH in humans has a half-life of roughly 20 to 30 minutes [5] and is cleared by the liver and kidneys.

GH secretion is primarily controlled by two hypothalamic neuropeptides, growth hormone-releasing hormone (GHRH) and somatostatin (SST). GHRH stimulates GH gene transcription and hormone release from the somatotrophs in the anterior pituitary, while SST maintains a tonic inhibitory tone [6, 7]. GH levels are also influenced by age,

• J. X. Genty is with the Department of Electrical and Computer Engineering at the University of Houston, Houston, TX 77004 USA. Email: jxgenty@uh.edu

sex, diet, exercise, time of day, stress, and sleep/wake states [8, 9, 10, 11, 6]. These factors modulate GH concentration through effects on both GH pulse amplitude and frequency [6, 12].

In men, sleep-associated pulses contribute to roughly 70% of daily GH output; the GH pulse at sleep-onset is generally the largest amplitude pulse observed over a 24-hour ("diurnal") period [13, 14]. While sleep-associated pulses also occur in women, they typically account for only a small proportion of total daily GH production [13, 14]. A number of observational and interventional studies in human participants have shown that GH secretion is temporally associated with, and may be stimulated by, "deep" or slow-wave sleep (SWS, stage N3 of non-REM sleep) [13, 15].

Previous studies of GH data usually used one of two classes of methods to report metrics: GH concentration peak detection (to identify a pulse) via cluster analysis as in [10, 11] or a parameter sweep based on initial predictions and subsequent refitting as in [6]. While methods of peak detection can roughly estimate the number of GH pulses, these methods struggle to identify statistically significant peaks in cases where degradation after one pulse is incomplete before the subsequent pulse occurs. Additionally, peak detection methods suffer in situations where GH amplitudes are so low that the observed data are susceptible to Gaussian noise. Peak detection methods also cannot recover underlying model parameters related to the infusion, clearance and basal secretion rates of GH. The parameter sweep approach to model fitting for GH requires initial guessing of secretory event locations from a plot of the

M. R. Amin is with the Department of Electrical and Computer Engineering at the University of Houston, Houston, TX 77004 USA. Email: mamin@uh.edu

N. D. Shaw is with the Clinical Research Branch at the National Institute
of Environmental Health Sciences, National Institutes of Health, Research
Triangle Park, NC 27709 USA. Email: natalie.shaw@nih.gov

[•] E. B. Klerman is with the Department of Neurology at Massachusetts General Hospital Boston, MA 02114 USA, the Department of Medicine at Brigham and Women's Hospital, Boston, MA 02115 USA and Harvard Medical School, Boston, MA 02115 USA. Email: ebklerman@hms.harvard.edu

R. T. Faghih is with the Department of Electrical and Computer Engineering at the University of Houston, TX 77004 USA. Email: rtfaghih@uh.edu

observed data. This method, of guessing and checking until a suitable fit is reached, is time-consuming and lacks a systematic approach. We develop an algorithm that accurately estimates the timing and amplitude of GH pulses in order to investigate the relationship between GH pulses and sleep. To test this new method, we use GH data collected during overnight frequent blood sampling studies from 18 adolescent participants.

We adopt a model of GH secretion similar to that proposed by Klerman et al. [6]. We apply a deconvolution algorithm, similar to those proposed by Faghih et al. [16, 17, 18, 19] for cortisol data and later extended by Amin et al. [20] for skin conductance signals, to analyze serum GH levels. This deconvolution method recovers the timing and amplitude of hormonal secretory events using a sparse recovery method and estimates model parameters with an interior point method. A coordinate descent approach combines the previously described methods to iteratively estimate sparse secretory events and model parameters. We also implement generalized cross-validation, as in [18], to recover the accurate number of hormone pulses while maintaining a balance between the sparsity and residual error of the estimate.

2 Methods

2.1 Experiment

In both experiments, serum GH levels were measured in blood samples collected every 10 minutes for 8 hours through a peripheral intravenous catheter (PIVC) during scheduled overnight sleep sessions. Each participant therefore contributed 49 data points. Information on participant sex, age, body mass index (BMI) and Apnea-Hypopnea Index (AHI) is included in the Supplemental Information. Sleep was recorded by polysomnography using established techniques [21]. GH was assayed from participant blood samples using the Roche Elecsys E170 immunoassay platform, with an interassay and total imprecision coefficient of variance (CV) of 0.6-1.7% and 1.7-4.1%, respectively [22].

- 1) Dataset 1: 14 adolescents, ages 11.3 to 14.1 years, 50% male, with no chronic medical conditions.
- 2) Dataset 2: 4 adolescents, ages 11.8 to 14.4 years, 75% male, with very mild obstructive sleep apnea (OSA). OSA is a condition characterized by the repetitive obstruction of the upper airway during sleep, causing episodic hypoxemia followed by awakening/arousal, and is often associated with daytime sleepiness [23]. Mild pediatric OSA is defined as an apnea-hypopnea index (AHI) greater than 1 and less than or equal to 5 [24]. During scheduled sleep, the participants used a continuous positive airway pressure (CPAP) machine to treat their OSA, facilitating an undisturbed sleep session similar to the participants from Da-

2.2 Model Formulation

We build a model based on the two-dimensional linear differential equations proposed by Klerman et al. [6], describing diurnal GH secretion. Originally, this model included feedback, due to the inhibitory effect of GH on GH release [25]; this effect occurs at the hypothalamic level

through a short loop mechanism, inhibiting GHRH and stimulating the release of SST into peripheral circulation [6]. However, the model we propose does not include GH negative feedback, because of (i) feedback's insignificant and/or erroneous effect on model fits [6], (ii) feedback decreases the parsimony of the system, and (iii) Klerman et al. [6] noted that GH secretion model fits were graphically indistinguishable with or without negative feedback. We model the dynamics of GH secretion with the following two-dimensional linear differential equations:

$$\frac{dh_1(t)}{dt} = -\beta_I h_1(t) + u(t) \tag{1}$$

$$\frac{dh_1(t)}{dt} = -\beta_I h_1(t) + u(t) \tag{1}$$

$$\frac{dh_2(t)}{dt} = \beta_I h_1(t) - \beta_C h_2(t) \tag{2}$$

where $h_1(t)$ represents the releasable GH in the anterior pituitary and $h_2(t)$ represents the GH concentration in the peripheral serum. β_I and β_C represent the GH infusion rate from the pituitary and GH clearance rate by the kidneys and liver, respectively. u(t) corresponds to the hypothalamic pulses that stimulate GH secretion where u(t) = $\sum_{i=1}^{N} q_i \delta(t-\tau_i)$ [18]. Finally, we assume that pulses occur at integer minute values. In this abstraction of hormone pulses, q_i represents the amplitude of the hormone pulse, τ_i represents the pulse timing and N represents the length of the input (N = 481). If q_i is zero, then a pulse did not occur at time τ_i .

TABLE 1 ESTIMATED INFUSION, CLEARANCE AND BASAL SECRETION RATES, NUMBER OF SECRETORY EVENTS AND THE SQUARES OF THE MULTIPLE CORRELATION COEFICIENTS (R^2) FOR THE FITS OF THE OBSERVED GH DATA FROM DATASET 1.

Participant	$\beta_I(\min^{-1})$	$\beta_{\mathcal{C}}(\text{min.}^{-1})$	$\rho\left(\frac{ng}{ml}\right)$	N	R^2
1-1	0.17	0.03	0.06	7	0.95
1-2	0.12	0.09	0.19	8	0.93
1-3	0.12	0.05	0.04	4	0.96
1-4	0.16	0.11	0.10	11	0.87
1-5	0.19	0.10	0.10	7	0.93
1-6	0.04	0.03	0.00	8	0.99
1-7	0.16	0.11	0.48	10	0.88
1-8	0.05	0.04	0.00	6	0.96
1-9	0.14	0.27	0.48	8	0.96
1-10	0.15	0.14	0.39	5	0.88
1-11	0.06	0.04	0.23	5	0.91
1-12	0.06	0.04	0.00	6	0.93
1-13	0.14	0.03	1.96	7	0.96
1-14	0.05	0.03	0.00	11	0.92
Median	0.13	0.05	0.10	7	0.93

Therefore, beginning at y_{t_0} , we have GH samples at 10minute intervals for M samples (M = 49) for each partici-

pant. Let
$$y_{t_{10}}, y_{t_{20}}, \dots, y_{t_{10M}}$$

$$y_{t_k} = h_2(t_k) + \rho + v_{t_k}$$
(3)

where y_{t_k} represents the serum GH level, ρ represents the time-invariant basal secretion rate of GH and v_{t_k}

represents the measurement error; missing data points are removed listwise, with a maximum of two samples missing from a participant. A description and discussion of listwise deletion rationale and method is provided in the Supplemental Information. We apply a least squares approach in our estimation algorithm, modelling v_{t_k} as a Gaussian random variable. Using the serum GH level (h_2) with a sampling interval of 10 minutes, we estimate β_1 , β_C , ρ , the number of secretory pulses and their corresponding timing and amplitude, with a 1 minute resolution.

TABLE 2

ESTIMATED INFUSION, CLEARANCE AND BASAL SECRETION RATES, NUMBER OF SECRETORY EVENTS AND THE SQUARES OF THE MULTIPLE CORRELATION COEFICIENTS (R^2) FOR THE FITS OF THE OBSERVED GH DATA FROM DATASET 2.

Participant	$\beta_I(\text{min.}^{-1})$	$\beta_{\mathcal{C}}(\text{min.}^{-1})$	$\rho\left(\frac{ng}{ml}\right)$	N	R^2
2-1	0.09	0.05	0.07	5	0.91
2-2	0.05	0.04	0.00	5	0.92
2-3	0.06	0.04	0.07	6	0.96
2-4	0.17	0.06	0.62	11	0.93
Median	0.08	0.04	0.07	5.5	0.93

2.3 Multi-Rate State-Space Formulation

In order to estimate the model parameters and determine the timing and amplitude of secretory pulses, we perform our deconvolution in the discrete time domain, as described by Amin *et al.* [20]. We reformulate (1, 2) by letting $[-\beta_1, 0]$

$$h(t) = \begin{bmatrix} h_1 & h_2 \end{bmatrix}^T, A_C = \begin{bmatrix} -\beta_I & 0 \\ \beta_I & -\beta_C \end{bmatrix},$$

 $B_C = \begin{bmatrix} 1 \\ 0 \end{bmatrix}$, and $C_C = \begin{bmatrix} 0 \\ 1 \end{bmatrix}$. Hence the state-space model can be written as:

$$\dot{h}(t) = A_C h(t) + B_C u(t)$$
 (4)
 $y(t) = C_C h(t) + \rho + v(t)$ (5)

where y(t) is the observed serum GH level and v(t) is the measurement noise at time t. Assuming that the inputs and the states are continuous over T_u , we let $\Lambda = e^{aT_u}$, and $\Gamma = \int_0^{T_u} e^{a(T_u - s)} ds$, we can write the discrete state-space

Participant 1 - 1

Participant 1 - 1

Participant 1 - 1

Republication of the property of the

form as:

$$h[k+1] = \Lambda h[k] + \Gamma u[k]$$
 (6)

$$y[k] = C_C h[k] + \rho + v[k]. \tag{7}$$

We let the blood sampling frequency $T_y = LT_u$, where L is an integer (L = 10 in this study). If we let $A_d = \Lambda^L$, $B_d = \begin{bmatrix} \Lambda^{L-1}\Gamma & \Lambda^{L-2}\Gamma & \cdots & \Gamma \end{bmatrix}$,

 $u_d[k] = [u[Lk] \quad u[Lk+1] \quad \cdots \quad u[Lk+L-1]^T,$

 $v_d[k] = v[Lk]$ and $h_d[k] = h[Lk]$, then we can represent the multi-rate system as:

$$h_d[k+1] = A_d h_d[k] + B_d u_d[k]$$
 (8)

$$y[k] = C_C h_d[k] + \rho + v_d[k] \tag{9}$$

where A_d and B_d are functions of β_I and β_C . Using the state transition matrix and considering the causality of the system, we can write the system equation as:

$$y[k] = F[k]h_d[0] + D[k]\mathbf{u} + \mathbf{\rho} + v_d[k]$$
 (10)

where
$$F[k] = C_c A_d^k$$
, $D[k] = C_c \begin{bmatrix} A_d^{k-1} B_d & A_d^{k-2} B_d & \cdots & B_d & \underbrace{0 & \cdots & 0}_{N-kL} \end{bmatrix}$,

$$\mathbf{F}_{\beta} = [F[0] \quad F[1] \quad \cdots \quad F[M-1]]_{M \times 2}^T,$$

$$\mathbf{D}_{\beta} = [D[0] \quad D[1] \quad \cdots \quad D[M-1]]_{M \times N}^T, \quad \text{and}$$

$$\mathbf{v} = [v[1] \quad v[2] \quad \cdots \quad v[M]]_{M \times 1}^T. \text{ Therefore, we can represent this system as:}$$

$$\mathbf{y} = \mathbf{F}_{\beta} H_d[0] + \mathbf{D}_{\beta} \mathbf{u} + \mathbf{\rho} + \mathbf{v}. \tag{11}$$

2.4 Estimation

We cast the system from (11) as the following least-squares optimization problem:

minimize
$$\frac{1}{2} \|\mathbf{y} - \mathbf{F}_{\beta} H_d[0] - \mathbf{D}_{\beta} \mathbf{u} - \boldsymbol{\rho} \|_2^2$$
 (12)

However, a least-squares solution for an underdetermined system could yield an incorrect estimation, as any given hormone assay can be erroneous. Moreover, the optimization problem is non-convex with respect to the parameters β_{I} , β_{C} , and ρ [18]. Some of these potential solutions may be outside of physiologically bounds,

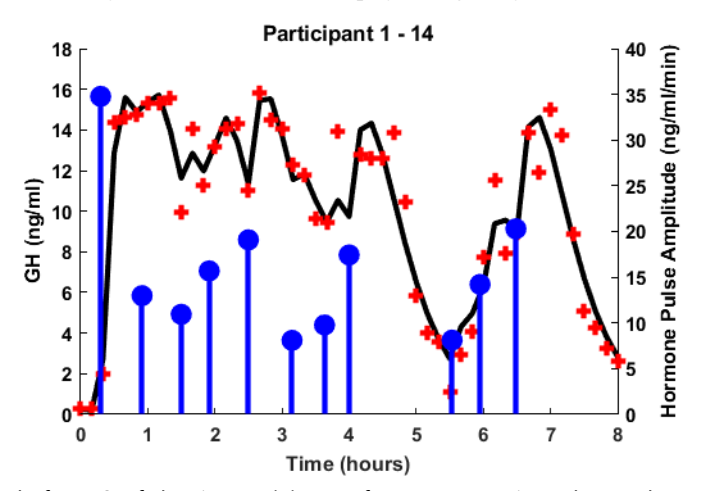


Figure 1. Estimated deconvolution of experimental 8-hour GH levels from 2 of the 14 participants from Dataset 1. Each panel shows the observed 8-hour GH time series (red crosses), the model-estimated GH levels (black curve), and the model-estimated pulse timing and amplitude (blue vertical lines) for a single participant. The estimated model parameters are provided in Table 1.

necessitating the implementation of GH specific constraints. We apply problem constraints based on the observed minimal and maximal values of model parameters and the timing and amplitude of GH secretory events from similar GH studies.

In modeling GH secretion over a 24-hour period, Berg et al. [11] reported an average of 11 secretory events for men and 13 secretory events for women. Previous studies have also demonstrated that the frequency of secretory events increases at night [14, 11]. However, Klerman et al. [6] reported a maximum of 3 secretory events per sleep episode in 12 female participants. These discrepant findings for GH parameters may be due to differences in GH immunoassay platforms [26], different study populations [27], or other unknown factors. We use these experimental values from previous studies to guide the application of constraints, ensuring that the estimated number of secretory pulses is within physiologically plausible bounds. We select a constraint of 11 possible secretory events during a sleep episode, significantly more than the maximum of 3 secretory events observed by Klerman et al. [6]. Applying such a generous constraint allows our algorithm to estimate the number of secretory events within a broad range of values. As a result, we mitigate the underestimation of secretory events that could arise due to known or unknown differences between this study and previous GH studies. We assume that **u** contains at most 11 positive elements out of 490 possibilities ($0 \le ||\mathbf{u}||_0 \le 11$, $\mathbf{u} \ge 0$). We impose a sparsity constraint on u, to limit the number of predicted pulses. Additionally, we extend the bounds on β_I and β_C , provided by [6], from 8.333×10^{-4} and 0.1333 min^{-1} to 8.333×10^{-4} and 1 min⁻¹, because preliminary analyses, bounding β_I and β_C between 8.333×10^{-4} and 1 min⁻¹, yielded estimates of β_I and β_C always within bounds, which are appropriate.

We solve this optimization problem by reformulating (12), with model constraints, as follows:

minimize
$$J_{\lambda}(\boldsymbol{\beta}, \mathbf{u}) = \frac{1}{2} \| \mathbf{y} - \mathbf{F}_{\boldsymbol{\beta}} H_d[0] - \mathbf{D}_{\boldsymbol{\beta}} \mathbf{u} - \boldsymbol{\rho} \|_2^2 + \lambda \| \mathbf{u} \|_p^p (13)$$
 subject to $C\boldsymbol{\beta} \leq b$, $\mathbf{u} \geq 0$, $0 \leq \| \mathbf{u} \|_0 \leq 11$ where $\boldsymbol{\beta} = [\beta_I \quad \beta_C \quad \rho]$, $\boldsymbol{C} = \begin{bmatrix} 1 & 0 & -1 & 0 & 0 \\ 0 & 1 & 0 & -1 & 0 \\ 0 & 0 & 0 & 0 & -1 \end{bmatrix}$, $\boldsymbol{b} = [1 \quad 1 \quad -8.333 \times 10^{-4} \quad -8.333 \times 10^{-4} \quad 0]'$. λ

λ

TABLE 3 ESTIMATED INFUSION, CLEARANCE AND BASAL SECRETION RATES, NUMBER OF SECRETORY EVENTS AND THE SQUARES OF THE Multiple Correlation Coeficients (\mathbb{R}^2) for the Fits of the Simulated GH Data from Dataset 1 at a SNR of 20 dB.

Participant	$\beta_I(\text{min.}^{-1})$	$\beta_{\mathcal{C}}(\text{min.}^{-1})$	$\rho\left(\frac{\text{ng}}{\text{ml}}\right)$	N	R^2	$\frac{ \beta_I - \widehat{\beta_I} }{\beta_I}$ (%)	$\frac{ \beta_C - \widehat{\beta_C} }{\beta_C}$ (%)	$ ho - \hat{ ho} \left(\frac{\mathrm{ng}}{\mathrm{ml}}\right)$
1-1	0.17	0.03	0.00	7	0.996	0.29	12.3	0.06
1-2	0.22	0.06	0.12	8	0.995	74.8	35.6	0.06
1-3	0.12	0.05	0.06	5	0.991	6.98	2.61	0.02
1-4	0.16	0.09	0.07	10	0.896	2.72	15.8	0.03
1-5	0.19	0.09	0.07	11	0.980	0.30	5.88	0.02
1-6	0.04	0.03	0.08	8	0.999	2.81	0.06	0.08
1-7	0.15	0.11	0.46	9	0.987	8.00	4.16	0.02
1-8	0.05	0.03	0.00	6	0.998	1.56	9.15	0.00
1-9	0.26	0.15	0.46	10	0.994	82.4	44.3	0.02
1-10	0.20	0.11	0.28	9	0.999	32.0	24.8	0.11
1-11	0.11	0.03	0.08	6	0.986	72.8	28.6	0.14
1-12	0.05	0.04	0.00	6	0.993	5.71	8.36	0.00
1-13	0.12	0.03	1.24	10	0.997	13.9	2.85	0.71
1-14	0.05	0.03	0.00	11	0.999	1.97	2.21	0.00
Median	0.11	0.04	0.05	7.5	0.997	6.59	10.8	0.02

TABLE 4 ESTIMATED INFUSION, CLEARANCE AND BASAL SECRETION RATES, NUMBER OF SECRETORY EVENTS AND THE SQUARES OF THE MULTIPLE CORRELATION COEFICIENTS (\mathbb{R}^2) FOR THE FITS OF THE SIMULATED GH DATA FROM DATASET 2 AT A SNR OF 20 DB.

Participant	$\beta_I(\text{min.}^{-1})$	$\beta_{\mathcal{C}}(\text{min.}^{-1})$	$\rho\left(\frac{\text{ng}}{\text{ml}}\right)$	N	R^2	$\frac{ \beta_I - \widehat{\beta_I} }{\beta_I}$ (%)	$\frac{ \beta_C - \widehat{\beta_C} }{\beta_C}$ (%)	$ ho - \hat{ ho} \left(\frac{\text{ng}}{\text{ml}}\right)$
2-1	0.12	0.04	0.07	5	0.995	24.8	13.0	0.00
2-2	0.23	0.03	0.02	8	0.987	379	36.9	0.02
2-3	0.05	0.04	0.00	6	0.994	14.5	4.46	0.07
2-4	0.15	0.05	0.47	9	0.992	10.0	21.9	0.15
Median	0.08	0.04	0.01	5.5	0.998	13.4	12.4	0.06

represents the regularization parameter, facilitating a balance between the sparsity of the input and the residual error in the model-estimated levels of GH, such that significant pulses are captured, and noise is filtered out. The sparsity of **u** increases with λ . Furthermore, the term $\lambda \|\mathbf{u}\|_{p}^{p}$ with $0 \le p < 2$, from (13), encourages sparsity and curbs overfitting in the solution of **u**. The previously mentioned term from (13) allows us to perform sparse recovery within a range of sparsity levels. We apply an iterative coordinate descent approach until the model parameters converge:

$$\mathbf{u}^{(k+1)} = \underset{\mathbf{u} \ge 0}{\operatorname{arg\,min}} \ J_{\lambda}(\boldsymbol{\beta}^{(k)}, \mathbf{u}^{(k)})$$
 (14)

$$\mathbf{u}^{(k+1)} = \underset{\substack{\mathbf{u} \ge 0 \\ 0 \le \|\mathbf{u}\|_0 \le 11}}{\arg \min} J_{\lambda}(\boldsymbol{\beta}^{(k)}, \mathbf{u}^{(k)})$$
(14)
$$\boldsymbol{\beta}^{(k+1)} = \underset{\mathbf{C}\boldsymbol{\beta} \le \mathbf{b}}{\arg \min} J_{\lambda}(\boldsymbol{\beta}^{(k)}, \mathbf{u}^{(k+1)})$$
(15)

We solve the optimization problem in (13), using the FO-CUSS+ algorithm proposed by Murray in [28], such that u is nonnegative and has a maximum sparsity of n (n = 11). This algorithm adopts a heuristic approach for updating λ , which balances the sparsity of \mathbf{u} against the residual er- $\operatorname{ror} \|\mathbf{y}_{\beta} - \mathbf{D}_{\beta}\mathbf{u}\|_{2}$, where $\mathbf{y}_{\beta} = \mathbf{y} - \mathbf{F}_{\beta}H_{d}[0] - \boldsymbol{\rho}$. The FO-CUSS+ algorithm works as follows, for $r = 1, 2, 3, \dots, 30$:

1.
$$\mathbf{P}_{\mathbf{u}}^{(r)} = \operatorname{diag}(|\mathbf{u}_{i}^{(r)}|^{2-p})$$

2.
$$\lambda^{(r)} = \left(1 - \frac{\left\|\mathbf{y}_{\beta} - \mathbf{D}_{\beta}\mathbf{u}^{(r)}\right\|_{2}}{\left\|\mathbf{y}_{\beta}\right\|_{2}}\right) \lambda_{max}, \lambda > 0$$

3.
$$\mathbf{u}^{(r+1)} = \mathbf{P}_{\mathbf{u}}^{(r)} \mathbf{D}_{\boldsymbol{\beta}}^{\mathsf{T}} \left(\mathbf{D}_{\boldsymbol{\beta}}^{r} \mathbf{P}_{\mathbf{u}}^{(r)} \mathbf{D}_{\boldsymbol{\beta}}^{\mathsf{T}} + \lambda^{(r)} \mathbf{I} \right)^{-1} \mathbf{y}_{\boldsymbol{\beta}}$$

4.
$$\mathbf{u}_{i}^{(r+1)} \le 0 \to \mathbf{u}_{i}^{(r+1)} = 0$$

After completing more than half of the total iterations, if $\|\mathbf{u}^{(r+1)}\|_{0} > n$, select the largest n values from $\mathbf{u}^{(r+1)}$ and set the rest to zero

Independently, FOCUSS+ yields estimated values for **u**, and we estimate β using the interior point method, iteratively solving equations (14) and (15). FOCUSS+ estimates \mathbf{u} with 11 secretory events. However, $\boldsymbol{\beta}$ and \mathbf{u} should be updated with a λ that balances the residual error and sparsity of the model. For this, we implement the Generalized Cross-Validation (GCV) technique for the selection of a regularization parameter [29]. The GCV function is defined as the following:

$$G(\lambda) = \frac{L \| (\mathbf{I} - \mathbf{H}_{\lambda}) \mathbf{y}_{\beta} \|}{\left(\operatorname{trace} (\mathbf{I} - \mathbf{H}_{\lambda}) \right)^{2}},$$
 (16)

where L is the number of data points and H_{λ} is the influence matrix. For FOCUSS+ algorithm, we define H_{λ} as H_{λ} = $\mathbf{D}_{\beta}\mathbf{P}_{\mathbf{u}}^{(r)}\mathbf{D}_{\beta}^{\mathsf{T}}(\mathbf{D}_{\beta}\mathbf{P}_{\mathbf{u}}^{(r)}\mathbf{D}_{\beta}^{\mathsf{T}} + \lambda^{(r)}\mathbf{I})^{-\mathfrak{D}}$. The GCV-FOCUSS+ algorithm works as follows, for $r = 1, 2, 3, \cdots$:

1.
$$\mathbf{P}_{\mathbf{u}}^{(r)} = \operatorname{diag}(|\mathbf{u}_{i}^{(r)}|^{2-p})$$

2.
$$\mathbf{u}^{(r+1)} = \mathbf{P}_{\mathbf{u}}^{(r)} \mathbf{D}_{\boldsymbol{\beta}}^{\mathsf{T}} \left(\mathbf{D}_{\boldsymbol{\beta}} \mathbf{P}_{\mathbf{u}}^{(r)} \mathbf{D}_{\boldsymbol{\beta}}^{\mathsf{T}} + \lambda^{(r)} \mathbf{I} \right)^{-1} \mathbf{y}_{\boldsymbol{\beta}}$$
3.
$$\mathbf{u}_{i}^{(r+1)} \leq 0 \rightarrow \mathbf{u}_{i}^{(r+1)} = 0$$

3.
$$\mathbf{u}_{i}^{(r+1)} \le 0 \to \mathbf{u}_{i}^{(r+1)} = 0$$

4.
$$\lambda^{(r+1)} = \arg\min_{0 \le \lambda \le 0.01} G(\lambda)$$

Iterate until convergence

Using the GCV method in tandem with FOCUSS+, we find an optimal choice for λ at each iteration, such that noise is filtered out in the estimation of **u** and iterate between solving (14) and (15) until convergence. We propose the following algorithm for the deconvolution of GH data:

Algorithm 1 Deconvolution Algorithm

- Initialize $\tilde{\beta}^0$ by sampling two uniform random variables r and s on [8.333 × 10^{-4} , 1] and let $\tilde{\beta}^0 = [r, s, 0]'$
- for $l = 1, 2, 3, \dots, 30$ do
- Set $\tilde{\beta}$ equal to $\tilde{\beta}^{l-1}$; using FOCUSS+, solve for $\tilde{\mathbf{u}}^l$ by initializing the optimization problem in (14) at vector of all ones
- Set $\tilde{\mathbf{u}}$ equal to $\tilde{\mathbf{u}}^l$; using the interior point method, solve for $\tilde{\beta}^l$ by initializing the optimization problem in (15) at $\widetilde{\pmb{\beta}}^{l-1}$
- Initialize $\hat{\boldsymbol{\beta}}^0$ and $\hat{\boldsymbol{u}}^0$ by setting them equal to the $\hat{\boldsymbol{\beta}}^l$, \boldsymbol{u}^l and $\hat{\rho}^l$ that minimize $J_{\lambda}(\beta, \mathbf{u})$ in (13), and let m = 1
- while until convergence do
- Set $\hat{\boldsymbol{\beta}}$ equal to $\hat{\boldsymbol{\beta}}^{m-1}$; using GCV-FOCUSS+, solve for $\hat{\boldsymbol{u}}^m$ by initializing the optimization problem in (14) at $\hat{\mathbf{u}}^{m-1}$
- Set $\hat{\mathbf{u}}$ equal to $\hat{\mathbf{u}}^m$; using the interior point method, solve for $\hat{\beta}^m$ by initializing the optimization problem in (15) at $\hat{\mathbf{\beta}}^{m-1}$ m = m + 1
- 10: end while
- 11: Set the estimated model parameters β and input \mathbf{u} to the β and \mathbf{u} of the 64 potential solutions that minimize $J_{\lambda}(\boldsymbol{\beta}, \mathbf{u})$ in (13)

We account for the nonconvexity of this optimization problem by performing multiple and different initializations of model paramters at the beginning of the algorithm. Step 1 initializes β at random values within a physiologically plausible range. Steps 2-5 use FOCUSS+ for sparse recovery and interior point method for finding algorithm initial conditions. Step 6 finds a good initial condition for the coordinate descent portion of the algorithm. Steps 7-10 apply a coordinate descent approach, to estimate the timing and amplitude of secretory events and model parameters until said unknowns converge. We incorporate sparse recovery in our coordinate descent approach via GCV – FO-CUSS+. GCV – FOCUSS+ applies generalized cross-validation to find the regularization parameter that balances between capturing sparsity and noise. Finally, the model parameters that minimize the cost function in (13), among all initializations, are selected in step 11.

We ran the proposed algorithm, with GH-specific constraints, for 64 initializations for each 8-hour measurement of serum GH concentration, for both datasets (Tables 1 and 2). Data analysis and estimation were performed in MATLAB R2020a.

Using the model for GH secretion detailed in equations (1) and (2), we also simulate 18 (i.e., one per participant) 8hour GH time series with the model parameters from Tables 1 and 2 and the GH pulses from Figures S-1 and S-2 (in Supplemental Information file. Then, we add zero mean Gaussian noise, using a range of signal to noise ratios (SNR) from 5 to 50 dB, at intervals of 5 dB, to the simulated GH time series, using the observation model (3). Finally, we evaluate the performance of our algorithm in estimating model parameters and recovering hormone pulses at these noise levels. Each of these simulated data are sampled every 10 minutes.

3 RESULTS

The observed and model-estimated GH levels and the timing and amplitude of hormonal secretory events in two participants from the first of the two datasets analyzed are shown in Figure 1; the associated model parameters for each participant, from each data set, are detailed in Tables 1 and 2, respectively. The median value for the square of the multiple correlation coefficient (R^2) among all experimental datasets is 0.93, with only three datasets having an R^2 below 0.90. The timing and amplitude of the hormonal pulses and model parameters vary greatly among participants. A straight line in quantile-quantile plots of the measurement error in the estimation of experimental GH levels demonstrates the Gaussian nature of the noise present in a participant's data; this is observed in the quantile-quantile plot of one of three participants with a low R^2 , implying the probable role of Gaussian noise in producing a low R^2 value (Figure 2). However, slight deviations from a straight line in the quantile-quantile plots of other participants with low R² values, suggest a margin of improvement in our model. Larger deviations in the quantile-quantile plots of other participants, including those with satisfactory

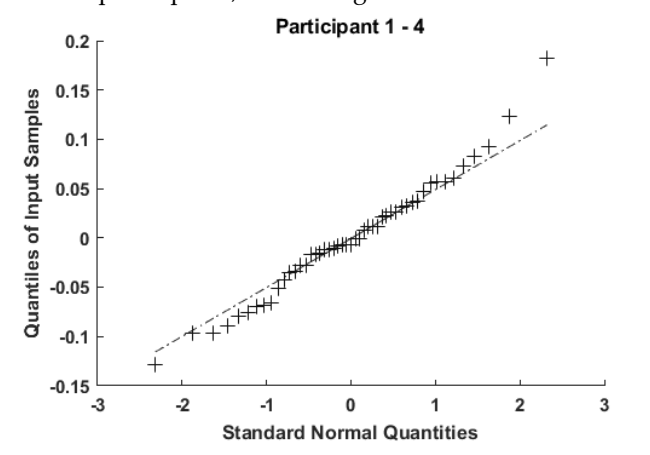
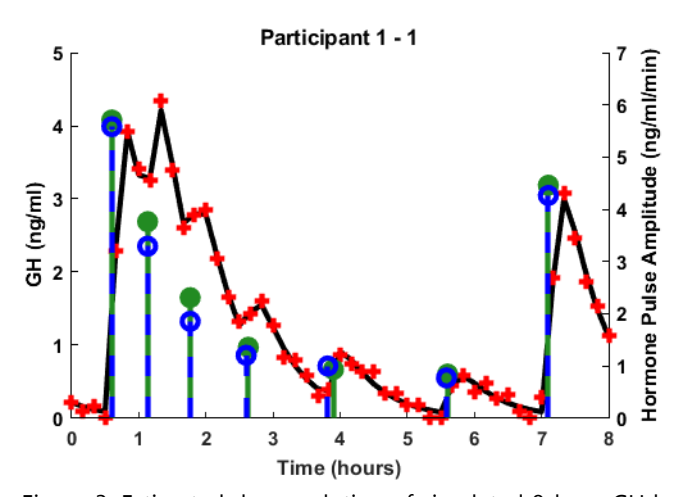


Figure 2. Quantile-Quantile plot of the measurement error in the estimation of Participant 1-4's observed GH levels.



 R^2 values, can be attributed to the combination of the low sampling rate of the experimental GH data and the small rise time of a participant's serum GH level. This small rise time reflects high frequency components in the GH signal, making the estimation of rise times difficult with a low sampling frequency.

The estimated model parameters, number of recovered pulses, the square of the multiple correlation coefficient (R^2) and the absolute difference and percentage error in the estimation of model parameters for the fits of the simulated GH data, at a SNR of 20 dB are detailed in Tables 3 and 4. The percent errors in the estimation of β_I and β_C range from small values (0.06% and 0.29%) to high values (379% and 82.4%), at a SNR of 20 dB. In some cases, the noise added to the simulated data is comparable in amplitude to the small GH pulses, facilitating a noticeable divergence in pulsatile patterns between experimental and simulated GH time series. The nonconvexity of this optimization problem ensures that differences in pulsatile patterns will also impact the estimation of timing and amplitude of GH pulses and model parameters. The actual sparse input, the estimated input and the simulated and estimated GH data, at a SNR of 20 dB for 2 of the 14 participants from Dataset 1 are in Figure 3. The estimated and simulated inputs are in good agreement, except at a higher noise level in which a few small amplitude pulses are ignored or noise is captured as a small pulse. For example, at a SNR of 20 dB there are ten such cases, but at 35 dB there are only four instances. The estimation of simulated inputs improves at lower noise levels, as indicated by Figure 4, which illustrates the average percent error in the estimation of l_0 –, l_1 –, and l_2 – norms of **u** at different levels of noise. Similarly, Figure 5 demonstrates the average percent error in the estimation of GH infusion and clearance rates decreasing from 0 to ~25 dB and then flattening out at around 20% error.

4 DISCUSSION

Our method successfully fit experimental and simulated

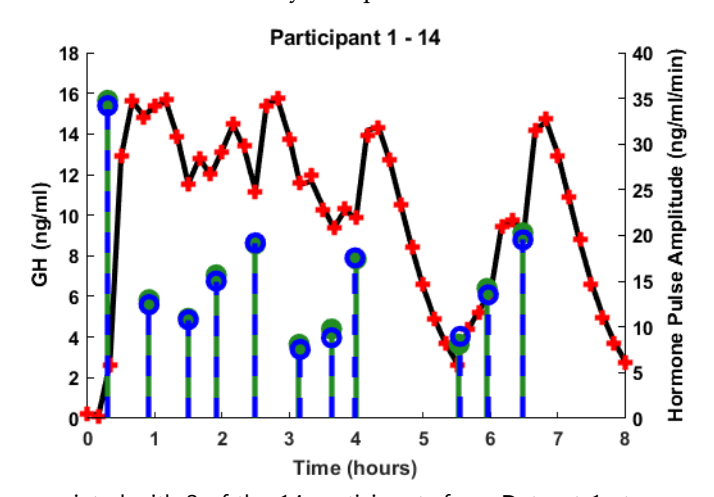


Figure 3. Estimated deconvolution of simulated 8-hour GH levels associated with 2 of the 14 participants from Dataset 1 at a SNR of 20 dB. Each panel shows the simulated 8-hour GH time series (red crosses) generated from the "ground truth" pulse timing and amplitude (forest green vertical lines), the model-estimated GH levels (black curve), and the model-estimated pulse timing and amplitude (blue vertical lines) for a single participant. The estimated model parameters are provided in Table 3.

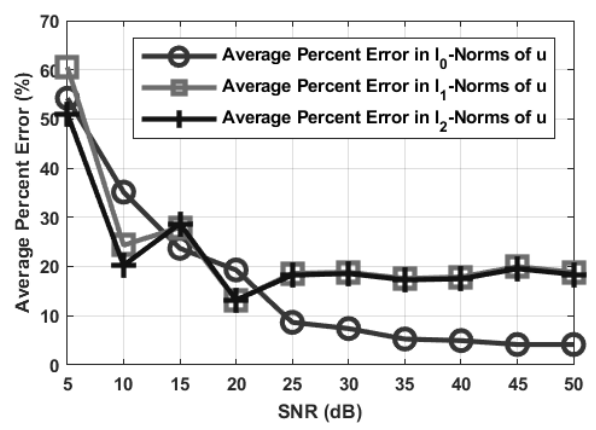


Figure 4. Average Percent Error in the l_0 –, l_1 – and l_2 –Norms of ${\bf u}$ vs. SNR (dB). The red circles correspond to the average percent error in the l_0 -norms of ${\bf u}$, the green squares correspond to the average percent error in the l_1 -norms of ${\bf u}$ and the blue crosses correspond to the average percent error in the l_2 -norms of ${\bf u}$.

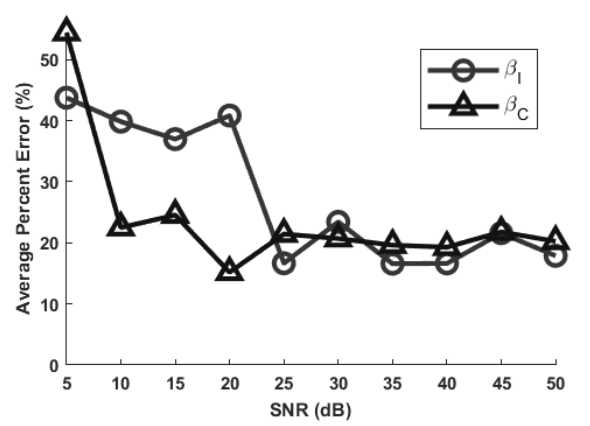


Figure 5. Average Percent Error in the Estimation of GH Infusion (β_I) and Clearance (β_C) Rates vs. SNR (dB).

GH data from 18 participants: 14 healthy adolescents and 4 adolescents with mild OSA who used a CPAP machine during sleep.

From our analysis of these 18 experimental sleep episodes, we identified an average of 7 hormonal secretory events per episode. This is greater than twice the average number of secretory events observed by Klerman *et al.* [6] and by Nindl *et al.* [30] and nearly half the number observed by Ho *et al.* [10] and Berg *et al.* [11] using data from healthy adults. Additionally, we found the the average estimated GH infusion and clearance rates are 0.11 min.⁻¹ and 0.07 min.⁻¹, respectively; Klerman *et al.* [6] observed average GH infusion and clearance rates of 0.02 min.⁻¹ for both parameters. The variations of the model parameters and number of secretory events between studies is most likely due to the different ages of the study populations [27].

We hypothesize that the $R^2 < 0.90$ in at least one of four participant's experimental datasets is due to the Gaussian noise present in those particular blood samples. The quantile-quantile plot displayed in Figure 3 demonstrate the Gaussian nature of the noise present in the observed GH signal, making the estimation of model parameters and

hormone pulses difficult for our sparse recovery algorithm. The CVs of the Elecsys GH immunoassay indicate that the GH data collected are likely both reproducible and robust. However, we do not have the standard deviations of noise related to the GH assay used in this experiment. As a result, we simulated GH data at ten different noise levels to evaluate the performance of our algorithm. If we had the noise levels for each GH assay performed, then we could simulate GH data with comparable noise levels to the experimental one.

The algorithm produces accurate estimations of model parameters for noise levels less than 20 dB (Figures 4 and 5). At a SNR greater than or equal to 20 dB, our algorithm performed well on most simulated GH data, with less than 20% error on average in the estimation of model parameters. Nevertheless, the nonconvexity of the optimization problem and the existence of many local minima can cause our algorithm to converge to a solution other than the ground-truth and produce a large error in the estimation of model parameters. At a SNR of 20 dB, there is a single outlier of 379% error in the estimation of the GH infusion rate. While the GH infusion and clearance rates are constrained to physiologically plausible values, the lower bound is close to zero, yielding model-estimated parameters close to zero in some cases. Therefore, a small absolute error can lead to a large pergentage error. For example, the absolute error, in this instance, is 0.19 min.⁻¹, producing a percentage error of 379%, as the ground-truth GH infusion rate is 0.05 min.⁻¹. There are several potental ways to improve the estimation of model parameters and the timing and amplitude of hormone pulses: (i) reducing the error introduced by the GH assay procedure itself and (ii) increasing the sampling rate of GH data, since the rise time of a GH pulse is shorter than its decay, meaning that our estimation algorithm has less data to estimate the GH infusion rate than the clearance rate. If a system for noninvasive and continuous sampling (such as exists for cortisol [31]) were available for GH, then GH detection with a higher sampling frequency might improve estimation.

5 CONCLUSION AND FUTURE WORK

In this study, we have demonstrated a robust method for the deconvolution of serum GH data to obtain physiologically important metrics by formulating an optimization problem to recover model parameters and GH pulses with physiologically plausible constraints.

We proposed a two-step coordinate descent approach, incorporating sparse recovery for GH secretory events and the interior point method for model parameters. We also implemented GCV to obtain regularization parameters, balancing the residual error against the sparsity of GH secretory events. Finally, we demonstrated the effectiveness of a previously used (on other pulsatile hormone data sets) sparse recovery framework for GH.

Using these methods, we can, in future studies, examine the relationship between GH pulse onset and/or pulse amplitude with sleep stage or other physiological events and the effect of sleep disruption, other physiological events, or clinical or other interventions on GH secretory parameters in different ages and populations and in normal and pathophysiological states.

ACKNOWLEDGMENT

This work was supported, in part, by NSF grants 1755780 CRII: CPS: Wearable-Machine Interface Architectures and 1942585 CAREER: MINDWATCH: Multimodal Intelligent Noninvasive brain sate Decoder for Wearable Adaptive Closed-loop architechtures. This work was also supported, in part, by the Intramural Research Programs of the NIH, National Institute of Environmental Health Sciences (Z01-ES103315) and by Grant Number 1UL1TR001102. NDS is also supported as a Lasker Clinical Research Scholar (1SI2ES025429-01). EBK is supported by NIH K24-HL105664 and P01-AG009975.

REFERENCES

- [1] S. Hiller-Sturmhöfel and A. Bartke, "The Endocrine System: An Overview," *Alcohol Health and Research World*, vol. 22, no. 3, pp. 153-162, 1998.
- [2] Y. Kato, Y. Murakami, M. Sohmiya and M. Nishiki, "Regulation of Human Growth Hormone Secretion and its Disorders," *Internal Medicine*, vol. 41, no. 1, pp. 7-13, 2002.
- [3] N. Møller and J. O. L. Jørgensen, "Effects of Growth Hormone on Glucose, Lipid, and Protein Metabolism in Human Subjects," *Endocrine Reviews*, vol. 30, no. 2, pp. 152-177, 2009.
- [4] S. Kim and M. Park, "Effects of growth hormone on glucose metabolism and insulin resistance in human," *Annals of Pediatric Endocrinology & Metabolism*, vol. 22, pp. 145-152, 2017.
- [5] P. E. Mullis, B. R. Pal, D. R. Matthews, P. C. Hind-marsh, P. E. Phillips and D. B. Dunger, "Half-life of exogenous growth hormone following suppression of endogenous growth hormone secretion with so-matostatin in type I (insulin-dependent) diabetes mellitus," *Clinical Endocrinology*, vol. 36, no. 3, 1992.
- [6] E. B. Klerman, G. K. Adler, M. Jin, A. M. Maliszewski and E. N. Brown, "A statistical model of diurnal variation in human growth hormone," *American Journal* of *Physiology*, vol. 285, no. 5, pp. E1118-E1126, 2003.
- [7] K. Gunawardane, T. K. Hansen, N. Muller, J. S. Christiansen and J. O. L. Jorgensen, "Normal Physiology of Growth Hormone in Adults," NCBI, 12 November 2015. [Online]. Available: https://www.ncbi.nlm.nih.gov/books/NBH279056. [Accessed 2 July 2019].
- [8] J. D. Veldhuis and A. Iranmanesh, "Physiological Regulation of the Human Growth Hormone (GH)-Insulin-Like Growth Factor Type I (IGF-I) Axis: Predominant Impact of Age, Obesity, Gonadal Function, and Sleep," American Sleep Disorders Association and Sleep Research Society, vol. 19, no. 10, pp. S221-S224, 1996.

- [9] F. Kimura and C. W. Tsai, "Ultradian rhythm of growth hormone secretion and sleep in the adult male rat," *The Journal of Physiology*, vol. 353, pp. 305-315, 1984.
- [10] K. Y. Ho, J. D. Veldhuis, M. L. Johnson, R. Furlanetto, W. S. Evans, K. G. M. M. Albert and M. O. Thorner, "Fasting Enhances Growth Hormone Secretion and Amplifies the Complex Rhythms of Growth Hormone Secretion in Man," *The American Society for Clinical Investigation, Inc.*, vol. 81, pp. 968-975, 1988.
- [11] G. V. D. Berg, M. F. J. D. Veldhuis and F. Roelfsema, "An Amplitude-Specific Divergence in the Pulsatile Mode of Growth Hormone (GH) Secretion Underlies the Gender Difference in Mean GH Concentrations in Men and Premenopausal Women," *Journal of Clinical Endocrinology and Metabolism*, vol. 81, no. 7, pp. 2460-2467, 1996.
- [12] M. L. Vance, J. Rivier and M. O. Thorner, "Pulsatile growth hormone secretion in normal man during a continuous 24-hour infusion of human growth hormone releasing factor (1-40). Evidence for intermittent somatostatin secretion.," *The Journal of Clinical In*vestigation, vol. 75, no. 5, pp. 1584-1590, 1985.
- [13] E. V. Cauter, L. Plat and G. Copinschi, "Interrelations Between Sleep and the Somatotropic Axis," *SLEEP*, vol. 21, no. 6, pp. 553-566, 1998.
- [14] E. V. Cauter and L. Plat, "SESSION III: SPONTANE-OUS GROWTH HORMONE SECRETION AND THE DIAGNOSIS OF GROWTH HORMONE DEFI-CIENCY," *The Journal of Pediatrics*, vol. 125, no. 5, Part 2, pp. S32-S37, 1996.
- [15] Y. Takahashi, D. M. Kipnis and W. H. Daughaday, "Growth Hormon Secretion during Sleep," *The Journal of Clinical Investigation*, vol. 47, no. 9, pp. 2079-2090, 1968.
- [16] R. T. Faghih, "From physiological signals to pulsatile dynamics: a sparse system identification approach," in *Dynamic Neuroscience*, Springer, 2018, pp. 239-265.
- [17] R. T. Faghih, "System identification of cortisol secretion," Massachusetts Institute of Technology, 2014.
- [18] R. T. Faghih, M. A. Dahleh, G. K. Adler, E. B. Klerman and E. N. Brown, "Deconvolution of Serum Cortisol Levels by Using Compressed Sensing," *PloS one*, vol. 9, no. 1, 2014.
- [19] R. T. Faghih, M.-F. M. P. A. Stokes, R. G. Zsido, S. Zorowitz, B. L. Rosenbaum, H. Song, M. R. Milad, D. D. Dougherty, E. N. Eskandar and e. al., "Characterization of Fear Conditioning and Fear Extinction by Analysis of electrodermal activity," in *Engineering in Medicine and Biology Society (EMBC)*, 2015 37th Annual International Conference of the IEEE, 2015.
- [20] M. R. Amin and R. T. Faghih, "Sparse Deconvolution of Electrodermal Activity via Continuous-Time System Identification," *IEEE Transactions on Biomedical Engineering*, 2019.
- [21] M. Marino, Y. Li, M. N. Rueschman, J. W. Winkelman, J. M. Ellenbogen, J. M. Solet, H. Dulin, L. F.

Berkman and O. M. Buxton, "Measuring Sleep: Accuracy, Sensitivity, and Specificity of Wrist Actrigraphy Compared to Polysomnography," *SLEEP*, vol. 36, no. 11, pp. 1747-1755, 2013.

- [22] J. Van Helden, D. Hermsen, N. Von Ahsen and M. Bidlingmaier, "Performance evaluation of a fully automated immunoassay for the detection of human growth hormone on the Elecsys immunoassay system.," *Clinical Laboratory*, vol. 60, no. 10, pp. 1641-1651, 2014.
- [23] M. Barnes, R. D. McEvoy, S. Banks, N. Tarquinio, C. G. Murray, N. Vowels and R. J. Pierce, "Efficacy of Positive Airway Pressure and Oral Appliance in Mild to Moderate Obstructive Sleep Apnea," *American Journal of Respiratory and Critical Care Medicine*, vol. 170, no. 6, 2004.
- [24] E. Dehlink and H. Tan, "Update on paediatric obstructive sleep apnoea," *Journal of Thoracic Disease*, vol. 8, no. 2, pp. 224-235, 2016.
- [25] R. Nass, A. A. Toogood, P. Hellmann, E. Bissonette, B. Gaylinn, R. Clark and M. O. Thorner, "Intracerebroventricular Administration of the Rat Growth Hormone (GH) Receptor Antagonist G118R Stimulates GH Secretion: Evidence for the Existence of Short Loop Negative Feedback of GH," *Journal of Neu*roendocrinology, vol. 12, pp. 1194-1199, 2000.
- [26] M. Bidlingmaier and P. Freda, "Measurement of human growth hormone by immunoassays: Current status, unsolved problems and clinical consequences," *Elsevier*, vol. 20, pp. 19-25, 2009.
- [27] Z. Zadik, S. A. Chalew, R. J. M. Jr., M. Meistas and A. A. Kowarski, "The influence of age on the 24-hour integrated concentration of growth hormone in normal individuals," *Journal of Clinical Endocrinology and Metabolism*, vol. 60, no. 3, pp. 513-6, 1985.
- [28] J. Murray, Visual Recognition, Inference and Coding Using Learned Sarse Overcomplete Representations, San Diego: University of California, 2005.
- [29] G. Golub, M. Heath and G. Wahba, "Generalized Cross-Vaidation as a Method for Choosing a Good Ridge Parameter," *Technometrics*, vol. 21, no. 2, pp. 215-223, 1979.
- [30] B. C. Nindl, W. C. Hymer, D. R. Deaver and W. J. Kraemer, "Growth hormone pulsality profile characteristics following acute heavy resistance exercise," *Journal of Applied Physiology*, pp. 163-172, 2001.
- [31] O. Parlak, S. T. Keene, A. Marias, V. F. Curto and A. Salleo, "Moleularly selective nanoporous membrane-based wearable organic electrochemical device fro noninvasive cortisol sensing," *Science Advances*, vol. 4, no. 7, 2018.
- [32] M. Nakai and W. Ke, "Review of Methods for Handling Missing data in Longitudinal Data Analysis," *International Journal of Mathematics Analysis*, vol. 5, pp. 1-13, 2011.
- [33] P. D. Allison, Missing Data Quantitative

applications in the social sciences, Thousand Oaks, CA: Sage, 2001.